Electron in a transverse harmonic cavity

H. Honkanen, P. Maris, J. P. Vary[1, *] and S. J. Brodsky[2, †]

[1] *Department of Physics and Astronomy, Iowa State University, Ames, Iowa 50011, USA*
[2] *SLAC National Accelerator Laboratory, Stanford University, Menlo Park, California, USA*
(Dated: August 3, 2010)

We employ Hamiltonian light-front quantum field theory in a basis function approach to solve the non-perturbative problem of an electron in a strong scalar transverse confining potential. We evaluate both the invariant mass spectra and the anomalous magnetic moment of the lowest state for this two-scale system. The weak external field limit of the anomalous magnetic moment agrees with the result of QED perturbation theory within the anticipated accuracy.

Physical systems with two or more distinct scales present a major computational challenge. Recent interest in strong field QED [1] has brought new emphasis on the need for robust methods for solving these problems. We address the problem of an electron in a transverse harmonic cavity and solve for its mass spectra and other observables as a function of the external field strength. To accomplish this, we evaluate the QED Hamiltonian on the light-front in a convenient basis with the Fock space consisting of electron states and an electron plus photon states. Our goal is to achieve results valid to leading order in QED for the electron's mass spectra and anomalous magnetic moment, $\delta\mu$, in a strong external scalar field treated non-perturbatively. The nonperturbative analysis presented in this paper could be applicable to measurements of the (gyromagnetic) ratio of the spin precession to Larmor frequencies of a trapped electron in strong external electromagnetic fields or intense time-dependent laser fields. This research also serves as a test case for using HO basis states for Hamiltonian light-front quantum field theories at strong coupling, such as the light-front QCD Hamiltonian in the nonperturbative domain. In this case the HO Fock state basis is supported by successful AdS/QCD models [2].

Adopting recently introduced methods [3], we quantize QED on the light-front using the light-front gauge. We add the harmonic oscillator potential in the transverse direction to confine the system in those directions. We define our light-front coordinates as $x^\pm = x^0 \pm x^3$, $x^\perp = (x^1, x^2)$, where the variable x^+ is light-front time and x^- is the longitudinal coordinate. We adopt $x^+ = 0$, the "null plane", for our quantization surface.

As in Ref. [3], our basis states consist of 2-D harmonic oscillator (HO) states, which are combined with discretized longitudinal modes, plane waves satisfying selected boundary conditions. The HO states are characterized by a principal quantum number n, orbital quantum number m and HO energy Ω. Working in momentum space, it is convenient to write the 2-D oscillator as a function of the dimensionless variable $\rho = $

$|p^\perp|/\sqrt{M_0\Omega}$, and M_0 has units of mass. The orthonormalized HO wavefunctions in polar coordinates (ρ, φ) are then given in terms of the Generalized Laguerre Polynomials, $L_n^{|m|}(\rho^2)$, by

$$\Phi_{nm}(\rho, \varphi) = \langle \rho\varphi | nm \rangle$$
$$= \sqrt{\frac{2\pi}{M_0\Omega}} \sqrt{\frac{2n!}{(|m|+n)!}} e^{im\varphi} \rho^{|m|} e^{-\rho^2/2} L_n^{|m|}(\rho^2), \quad (1)$$

with eigenvalues $E_{n,m} = (2n + |m| + 1)\Omega$. The HO wavefunctions have the same analytic structure in both coordinate and momentum space, a feature reminiscent of a plane-wave basis.

The longitudinal modes, ψ_k, in our basis are defined for $-L \le x^- \le L$ with periodic boundary conditions (PBC) for the photon and antiperiodic boundary conditions (APBC) for the electron:

$$\psi_k(x^-) = \frac{1}{\sqrt{2L}} e^{i\frac{\pi}{L}k x^-}, \quad (2)$$

where $k = 1, 2, 3, ...$ for PBC (we neglect the zero mode) and $k = \frac{1}{2}, \frac{3}{2}, \frac{5}{2}, ...$ for APBC. The full 3-D single-particle basis state is defined by the product form

$$\Psi_{k,n,m}(x^-, \rho, \varphi) = \psi_k(x^-)\Phi_{n,m}(\rho, \varphi). \quad (3)$$

Following Ref.[4] we introduce the total invariant mass-squared M^2 for the low-lying physical states in terms of a Hamiltonian H times a dimensionless integer for the total light-front momentum K

$$M^2 + P_\perp P_\perp \to M^2 + const = P^+ P^- = KH \quad (4)$$

where we absorb the constant into M^2. For simplicity, the transverse functions for both the fermion and the boson are taken as eigenmodes of the trap. The non-interacting Hamiltonian H_0 for this system is then defined by the sum of the occupied modes i in each many-parton state:

$$H_0 = 2M_0 P_c^-$$
$$= \frac{2M_0\Omega}{K} \sum_i \frac{2n_i + |m_i| + 1 + \bar{m}_i^2/(2M_0\Omega)}{x_i}, \quad (5)$$

where $\bar{m}_i$ is the mass of the parton i. The photon mass is set to zero throughout this work and the electron mass $\bar{m}_e$ is set at the physical mass 0.511 MeV in our non-renormalized calculations. We also set $M_0 = \bar{m}_e$.

The light-front QED Hamiltonian interaction terms we need are the fermion to fermion-boson vertex, given as

$$V_{e \to e\gamma} = g \int dx_+ d^2x_\perp \overline{\Psi}(x)\gamma^\mu \Psi(x) A_\mu(x)\bigg|_{x^+=0}, \qquad (6)$$

and the instantaneous fermion-boson interaction,

$$V_{e\gamma \to e\gamma} = \frac{g^2}{2} \int dx_+ d^2x_\perp \overline{\Psi}\gamma^\mu A_\mu \frac{\gamma^+}{i\partial^+} (\gamma^\nu A_\nu \Psi)\bigg|_{x^+=0}, \qquad (7)$$

where the coupling constant $g^2 = 4\pi\alpha$, and α is the fine structure constant taken to be $\alpha = \frac{1}{137.036}$ in this work. The non-spinflip vertex terms of Eq.(6) are $\propto gM_0\Omega$, whereas spinflip terms are $\propto g\sqrt{M_0\Omega}m_e$. Selecting the initial state fermion helicity in the single fermion sector always as "up" the process $e \to e\gamma$ is nonzero for 3 out of 8 helicity combinations, and the process $e\gamma \to e\gamma$ is nonzero only with all 4 spin projections aligned (2 out of 16 combinations). The resulting Hamiltonian matrix is thus sparse.

We implement a symmetry constraint for the basis by fixing the total angular momentum projection $J_z = M + S = \frac{1}{2}$, where $M = \sum_i m_i$ is the total azimuthal quantum number, and $S = \sum_i s_i$ the total spin projection along the x^- direction. For cutoffs, we select the total light-front momentum, K, and the maximum total quanta allowed in the transverse mode of each one or two-parton state, N_{max}, such that

$$\sum_i x_i = 1 = \frac{1}{K}\sum_i k_i, \qquad (8)$$

$$\sum_i 2n_i + |m_i| + 1 \le N_{max}, \qquad (9)$$

where, for example, k_i defines the longitudinal modes of Eq.(2) for the ith parton. Eq.(8) signifies total light-front momentum conservation written in terms of boost-invariant momentum fractions, x_i. Since we employ a mix of boundary conditions and all states have half-integer total K, we will quote K-values rounded downwards for convenience, except when the precise value is required.

In Fig.1 we show the eigenvalues (multiplied by K) for a non-renormalized light-front QED Hamiltonian given in Eqs.(5,6,7), with fixed $\Omega = 0.05$ MeV and simultaneously increasing K and N_{max}. The resulting dimension of the Hamiltonian matrix increases rapidly. For $N_{max} = K = 2, 10, 20$, the dimensions of the corresponding symmetric $d \times d$ matrices are $d = 2, 1670, 26990$, respectively.

The number of the single fermion basis states, considering all the symmetries, increases slowly with increasing $N_{max} = K$ cutoff. For $N_{max} = K = 2, 10, 20$ the
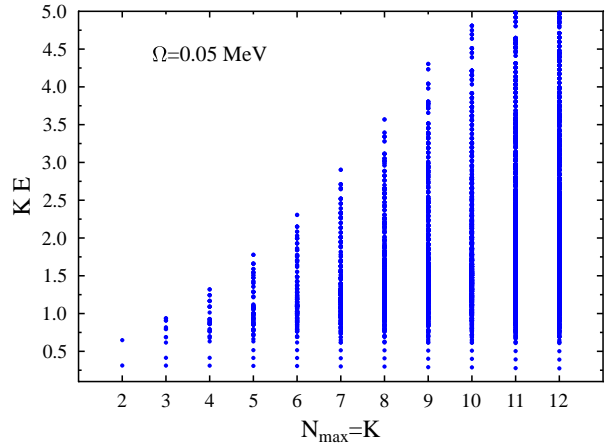

FIG. 1: Eigenvalues (multiplied by K) for a non-renormalized light-front QED Hamiltonian which includes the fermion-boson vertex and the instantaneous fermion-boson interaction without counterterms. The basis is limited to fermion and fermion-boson states satisfying the symmetries. The cutoffs for the basis space dimensions are selected such that K increases simultaneously with the N_{max}.

number of single fermion basis states is $1, 5, 10$, respectively. Our lowest-lying eigenvalue corresponds to a solution dominated by the electron with $n = m = 0$. The ordering of excited states, due to significant interaction mixing, does not always follow the highly degenerate unperturbed spectrum of Eq.(5). States dominated by spin-flipped electron-photon components are evident in the solutions. Nevertheless, the lowest-lying eigenvalues appear with nearly harmonic separations in Fig.1 as would be expected at the coupling of QED. The multiplicity of the higher eigenstates increases rapidly with increasing $N_{max} = K$ and the states exhibit stronger mixing with other states than the lowest-lying states. In principle the fermion-boson basis states interact directly with each other in leading order through the instantaneous fermion-boson interaction, but numerically the effect of this interaction is very weak, and thus does not contribute significantly to the mixing. Even though we work within a Fock space approach, our numerical results should thus approximate equal the lowest order perturbative QED results for sufficiently weak external field.

In Fig.2 we show the results for the square root of the electron anomalous magnetic moment (scaled), $\sqrt{\delta\mu/g^2}$, as a function of Ω obtained from the lowest mass eigenstate. That is, we plot the magnitude of the probability amplitude that electron has its spin flipped relative to the single electron Fock-space component in the range where the results are converged. Since our system is in an external field, the lowest physical mass eigenstate (not known experimentally) can deviate from the free electron mass. Therefore, before renormalization, we only consider cases where the mass eigenvalue falls within 25%
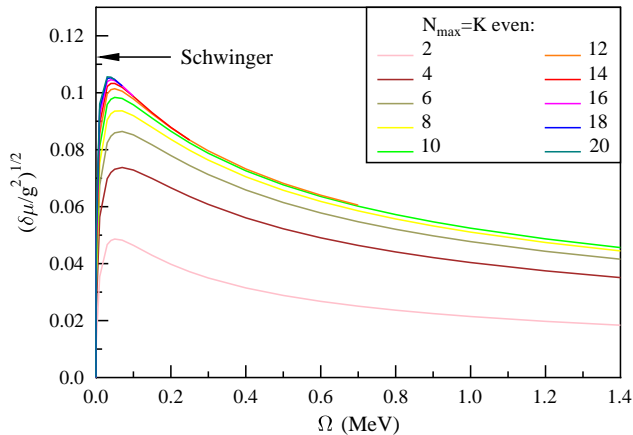
FIG. 2: (Color online) Square root of the (scaled) electron anomalous magnetic moment as a function of the transverse external field for a sequence of increasing basis spaces indicated in the legend. These are non-renormalized results where the mass eigenvalue falls within 25% of the free electron mass. The Schwinger result, appropriate to $\Omega = 0$ MeV, is indicated.
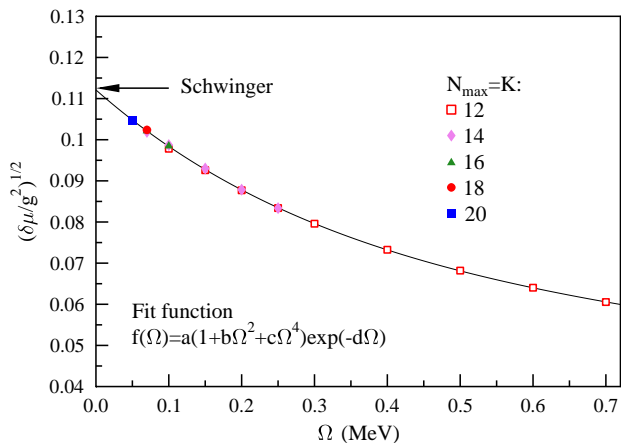

FIG. 3: (Color online) Fit to the results of Fig.2 for $N_{max} = K = 12, \ldots 20$. Extrapolation to zero external field yields 0.1121, compared with the theoretical 1-loop QED prediction ("Schwinger") of 0.1125.

of the free electron mass. At zero external field we may compare this result with the square root of the ratio of the Schwinger result $\frac{\alpha}{2\pi}$ to the coupling constant $g^2 = 4\pi\alpha$. For even $N_{max} = K$ the results converge rapidly for $N_{max} = K \geq 14$. The results for odd cutoffs (not shown) track even cutoff results as $N_{max} = K$ increases. Below $\Omega \lesssim 0.05$ MeV, in the weak external field region, all the interactions are quenched at fixed $N_{max} = K$, and not converged, due in part to our requirement that the HO basis states track the external field.

Fig.3 shows an extrapolation of the above results for $N_{max} = K = 12, \ldots, 20$ to the zero external field limit $\Omega = 0$ Mev. We have only included the points that have
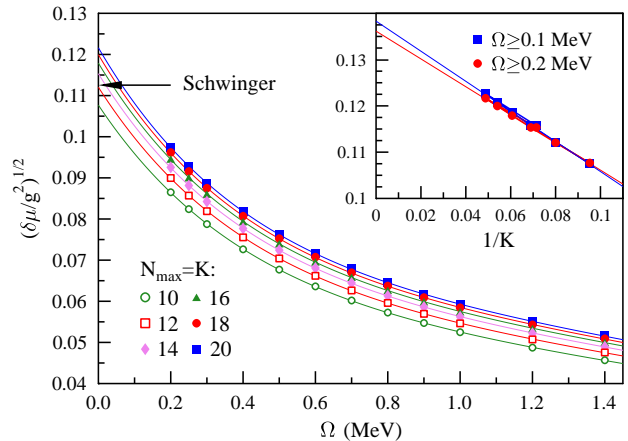

FIG. 4: (Color online) Individual fits to the renormalized results for square root of the (scaled) electron anomalous magnetic moment for $N_{max} = K = 10, \ldots, 20$. The inset shows the continuum limit extrapolation of the zero external field results in the main panel as a function of $1/K$.

$\Omega \gtrsim 0.05$ MeV, above the peak shown in Fig.2 where we have reasonable convergence. An excellent agreement with the results is obtained by a fit function $f(\Omega) = a(1 + b\Omega^2 + c\Omega^4)\exp(-d\Omega)$, with $a = 0.1121$. This is $< 1\%$ deviation from the Schwinger result of 0.1125, which is reasonable in light of our numerical accuracy and extrapolation uncertainties. If we perform individual extrapolations for all the $N_{max} = K = 12, \ldots, 20$ results with $0.1 \leq \Omega \leq 1.4$ MeV, a range spanning the electron mass scale, we obtain excellent fits with $0.1109 \leq a \leq 0.1134$, i.e. remaining within 1.5% of the Schwinger result.

In Ref.[3] we discussed possible divergences present in our framework, and anticipated a straightforward management of the identified divergences. Here we renormalize our results by applying a sector-dependent normalization scheme from Ref.[6]. In our present limited Fock space, we need only the mass counterterm δm_e. This δm_e is added to the mass term in the diagonal one-electron part of the Hamiltonian Eq.(5). In the absence of a known experimental mass for renormalization due to the external field, we adjust δm_e such that the lowest eigenstate remains at $KE_0 = m_e^2 + M_0\Omega$. That is, we simply adopt the free electron mass for the renormalized mass.

In Fig.4 we present $\sqrt{\delta\mu/g^2}$ for $N_{max} = K = 10, \ldots, 20$ from the renormalized QED Hamiltonian of Eq.(5), with δm_e, and Eqs.(6,7). To eliminate possible effects from the peak at $\Omega \sim 0.05$ MeV in Fig.2, we only include results with the external field $\Omega \geq 0.2$ MeV. Again, individual fits of the form $f(\Omega) = a(1 + b\Omega^2 + c\Omega^4)\exp(-d\Omega)$ are an excellent representation of our results. The range of the extrapolated values is $0.1077 \leq a \leq 0.1216$.

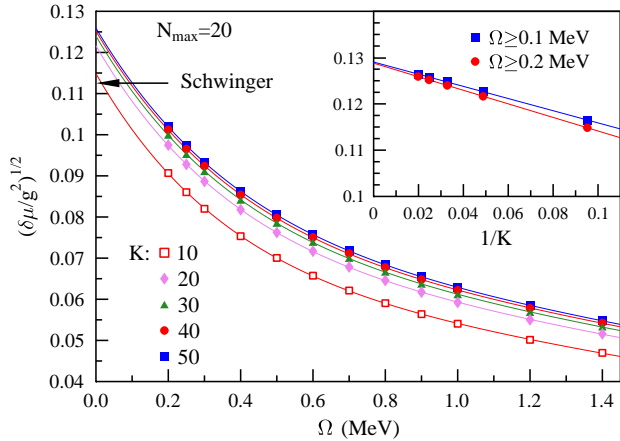The convergence with an increasing cutoff is now less

FIG. 5: (Color online) Individual fits to the renormalized results for square root of the (scaled) electron anomalous magnetic moment for $N_{max} = 20$, $K = 10, \ldots 50$. The inset shows the continuum limit extrapolation of the zero external field results in the main panel as a function of $1/K$.

rapid than in the non-renormalized case shown Fig.2. In order to approach the continuum limit $N_{max} = K \to \infty$, we perform further extrapolation to the zero-Ω results of Fig.4. The inset of Fig.4 shows linear extrapolation of the results of the main figure in $1/K$ to the continuum limit $N_{max} = K \to \infty$. To verify the stability of the results, an extrapolation based on the $\Omega \geq 0.1$ MeV fits (not shown) is also given. The extrapolated continuum values are 0.1362 (0.1383) for $\Omega \geq 0.2\,(0.1)$, respectively, and thus about 20% above the Schwinger result 0.1125. An enhancement of this magnitude was also observed in related works, Ref.[5] and Refs.[8, 9], where one-photon truncated light-front Hamiltonian was regulated with Pauli-Villars (PV) regularization scheme. With PV regularization as well as in our renormalized results, interpreted from a perturbation theory perspective, the intermediate state propogators are developed from a dynamical (non-perturbative) electron mass rather than using the unperturbed mass needed for direct comparison with perturbation theory.

In our approach the HO parameters Ω, M_0, the fermion mass m_e and the total longitudinal momentum K appear as prefactors for the matrix elements appearing in the Hamiltonian. Therefore we can rather straightforwardly vary the size of the Hamiltonian matrix by keeping N_{max} fixed, and changing K alone. In Fig.5 we study the continuum limit of $\sqrt{\delta\mu/g^2}$ by setting $N_{max} = 20$ and increasing K in units of 10, from $K = 10$ to $K = 50$. The dimension of the Hamiltonian matrix then increases

from $d = 11790$ to $d = 69590$. The extrapolated results in the main figure range between $0.1148 \leq a \leq 0.1259$, and show a good convergence pattern. The inset of Fig.5 shows linear extrapolation of the results of the main figure to the continuum limit $K \to \infty$. With $\Omega \geq 0.2\,(0.1)$ MeV the extrapolated values are 0.1288 (0.1290), $\sim 15\%$ above the Schwinger value.

In summary, we have evaluated properties of an electron in a non-perturbative external harmonic oscillator potential. We have taken the weak external field limit of the electron anomalous magnetic moment, and obtained results compatible with QED perturbation theory with reasonable accuracy. Our framework can be extended by incorporating higher Fock-space sectors and adopting external strong fields relevant to future high-intensity laser facilities. Applications to QCD will proceed with the adoption of recently-developed color-singlet basis enumeration techniques [3].

Acknowledgments.

The authors thank A. Harindranath, K. Tuchin, J. Hiller, S. Chabysheva, V. Karmanov and A. Ilderton for fruitful discussions. Computational resources were provided by DOE through the National Energy Research Supercomputer Center (NERSC). This work was supported in part by a DOE Grant DE-FG02-87ER40371 and by DOE Contract DE-AC02-76SF00515.

[*] Electronic address: heli, pmaris, jvary@iastate.edu
[†] Electronic address: sjbth@slac.stanford.edu
[1] C. K. Dumlu and G. V. Dunne, Phys. Rev. Lett. **104** (2010) 250402 [arXiv:1004.2509 [hep-th]], and references therein.
[2] G. F. de Teramond and S. J. Brodsky, Phys. Rev. Lett. **102**, 081601 (2009) [arXiv:0809.4899 [hep-ph]].
[3] J. P. Vary *et al.*, Phys. Rev. C **81**,(2010) 035205 [arXiv:0905.1411 [nucl-th]].
[4] S. J. Brodsky, H. C. Pauli and S. S. Pinsky, Phys. Rept. **301** (1998) 299 [arXiv:hep-ph/9705477].
[5] S. J. Brodsky, V. A. Franke, J. R. Hiller, G. McCartor, S. A. Paston and E. V. Prokhvatilov, Nucl. Phys. B **703** (2004) 333 [arXiv:hep-ph/0406325].
[6] V. A. Karmanov, J. F. Mathiot and A. V. Smirnov, Phys. Rev. D **77** (2008) 085028 [arXiv:0801.4507 [hep-th]].
[7] S. J. Brodsky, J. R. Hiller and G. McCartor, Phys. Rev. D **58**, 025005 (1998).
[8] S. S. Chabysheva and J. R. Hiller, arXiv:0911.3686 [hep-ph].
[9] S. S. Chabysheva and J. R. Hiller, Phys. Rev. D **81** (2010) 074030 [arXiv:0911.4455 [hep-ph]].